

RF-behavior optimization of GaN-based HFETs by coupled electrical-thermal simulation

R. Stenzel¹, J. Höntschel¹, W. Klix², A. Wieszt³, R. Behtash³ and H. Leier³

¹University of Applied Sciences Dresden, Friedrich-List-Platz 1, D-01069 Dresden, Germany, e-mail: stenzel@et.htw-dresden.de

²University of Technology Dresden, Mommsenstr. 13, D-01062 Dresden, Germany

³DaimlerChrysler AG, Research and Technology, Wilhelm-Runge-Str. 11, D-89081 Ulm, Germany

Abstract - The RF-behavior of AlGaIn/GaN-HFETs was investigated by numerical simulations to improve yield and device performance. Two-dimensional (2D) coupled electrical-thermal simulations have been carried out to study the influence of different device dimensions as well as layer doping and thickness. A new algorithm for the calculation of RF characteristics was developed to include external layout capacities and resistors. A model parameter calibration was done by experimental results of a Al_{0.25}GaN/GaN-HFET with 0.3 μm gate length. The variation of gate lengths in the range of 0.1 - 0.4 μm results in maximum frequencies of oscillation (f_{max}) between 80 GHz and 59 GHz.

Keywords: AlGaIn/GaN-HFET, electrical-thermal simulation, RF-behavior, polarization

1. INTRODUCTION

Significant progress has been made in the last few years in the development of GaN-based heterojunction field-effect transistors (HFETs) for high-speed, high-power and high-temperature applications. A quite number of investigations are necessary to improve yield and device performance. Numerical simulations have been carried out to study the influence of different device dimensions as well as layer doping and thickness.

An accurate prediction of the device characteristics requires an adjusted model and a calibration of the model parameters. Because of the notable self-heating effects in GaN-devices a coupled electrical-thermal simulation is accomplished. The influence of spontaneous and piezoelectric charges are taken into consideration. A new algorithm for the calculation of RF characteristics was developed to include external layout capacities and resistors, which is necessary for a good agreement with measured values.

2. SIMULATION MODEL

The numerical simulation is carried out by the 2D/3D-simulator SIMBA [1-3], based on a two- or three-dimensional coupled solution of Poisson equation

$$\nabla \cdot (\varepsilon \nabla \varphi) = -q(p - n + N_D^+ - N_A^- + \rho_{ADD}) \quad (1)$$

(φ electrostatic potential, p , n hole and electron densities, N_D^+ , N_A^- ionized donor and acceptor densities, ρ_{ADD} additionally fixed charge, ε permittivity)

the continuity equations for holes and electrons

$$\nabla \cdot \mathbf{J}_p = -q \cdot (R - G + \partial p / \partial t) \quad (2)$$

$$\nabla \cdot \mathbf{J}_n = q \cdot (R - G + \partial n / \partial t) \quad (3)$$

(\mathbf{J} current density, R recombination rate, G generation rate)

the corresponding transport equations

$$\mathbf{J}_p = -q\mu_p p \cdot \nabla(\varphi - \mathcal{O}_p) - \mu_p \cdot kT \cdot \nabla p \quad (4)$$

$$\mathbf{J}_n = -q\mu_n n \cdot \nabla(\varphi + \mathcal{O}_n) + \mu_n \cdot kT \cdot \nabla n \quad (5)$$

(μ_p , μ_n hole and electron mobility's, \mathcal{O}_p , \mathcal{O}_n hole and electron band parameters).

and the heat flow equation

$$\nabla \cdot (\lambda \cdot \nabla T) + H = \rho \cdot c \frac{\partial T}{\partial t} \quad (6)$$

with

$$H = \mathbf{J} \cdot \mathbf{E}^*, \quad \mathbf{E}^* = -\nabla(\varphi - \varphi_0) \quad (7)$$

(T lattice temperature, λ thermal conductivity, ρ density, c effective heat capacity)

High-order models like Schrödinger and energy balance equations are neglected in this case because of the high computation times.

From the results of static and dynamic simulation the calculation of small-signal parameters is possible. At the interesting operation point a dynamic simulation of a small voltage jump at the input and output terminal of the device will be done. The y-parameters as a function of frequency can be calculated by the recursive relations

$$Re\{y^{i+1}(\omega)\} = Re\{y^i(\omega)\} + \frac{\Delta I}{\Delta U} \left[\cos(\omega T^i) \cdot \frac{\sin(\omega \Delta t)}{\omega \Delta t} + \sin(\omega T^i) \cdot \frac{\cos(\omega \Delta t) - 1}{\omega \Delta t} \right] \quad (8)$$

$$Im\{y^{i+1}(\omega)\} = Im\{y^i(\omega)\} - \frac{\Delta I}{\Delta U} \left[\sin(\omega T^i) \cdot \frac{\sin(\omega \Delta t)}{\omega \Delta t} - \cos(\omega T^i) \cdot \frac{\cos(\omega \Delta t) - 1}{\omega \Delta t} \right] \quad (9)$$

(T_i time step i , Δt time step size, ΔI current variation, ΔU voltage jump)

Consequently an equivalent circuit can be created. External layout capacities (C_{gse} , C_{gde}) and a resistor (R_{ge}) are added (see Figure 1).

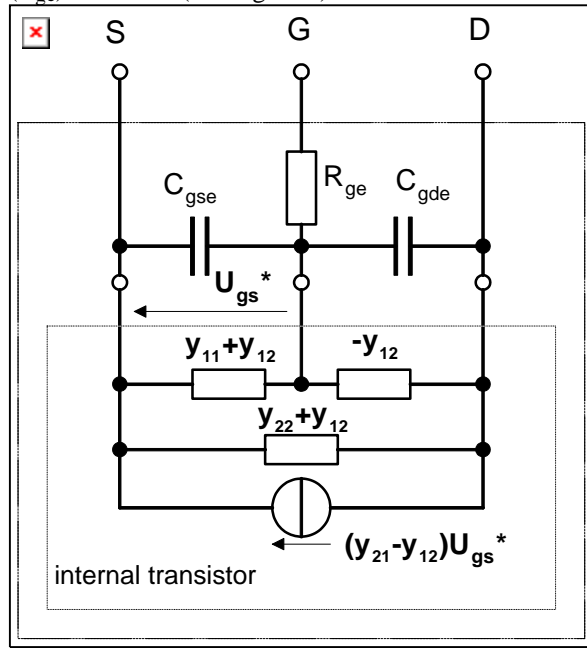


Figure 1: Equivalent circuit with external elements

From this the y -parameters of the completed device and consequently the RF-parameters current gain (h_{21}), maximum stable gain (MSG) and maximum available gain (MAG) as well as the transit frequency (f_t) and the maximum frequency of oscillation (f_{max}) can be calculated.

3. DEVICE STRUCTURE

The calculated $Al_{0.25}Ga_{0.75}N/GaN$ -HFET-structure is represented in Figure 2. The GaN buffer as well as the AlGaN barrier- and the cap-layers are unintentionally doped ($10^{16}cm^{-3}$ assumed). The supply layer is Si-doped ($5 \cdot 10^{18}cm^{-3}$). The effects of spontaneous and piezoelectric polarization are included by a positive interlayer charge $\sigma = 1.4 \cdot 10^{13}cm^{-2}$ [4] at the heterojunction interface.

The SiC substrate and the AlN nucleation layer are neglected at the electrical simulation whereas a corresponding thermal resistor is included during the solution of the heat flow equation.

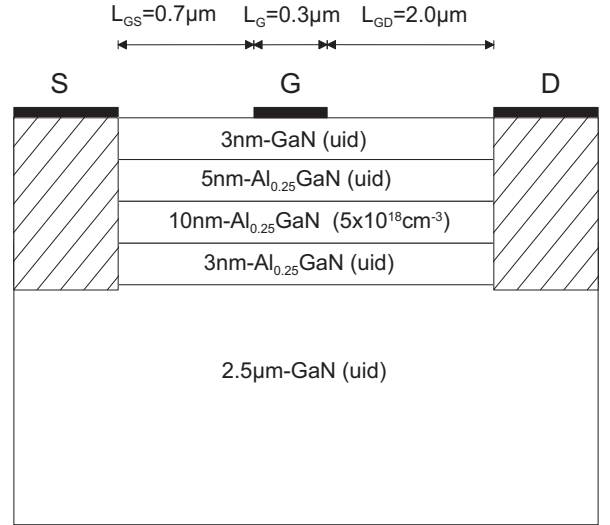


Figure 2: Device structure, used for simulations

Figure 2 shows the coplanar layout of a 2-finger HFET ($2 \times 50 \mu m$). The external layout capacities are estimated to $C_{gse} = 15$ fF, $C_{gde} = 11$ fF by numerical field simulations and the gate connection resistor is assumed to $R_{ge} = 30 \Omega$.

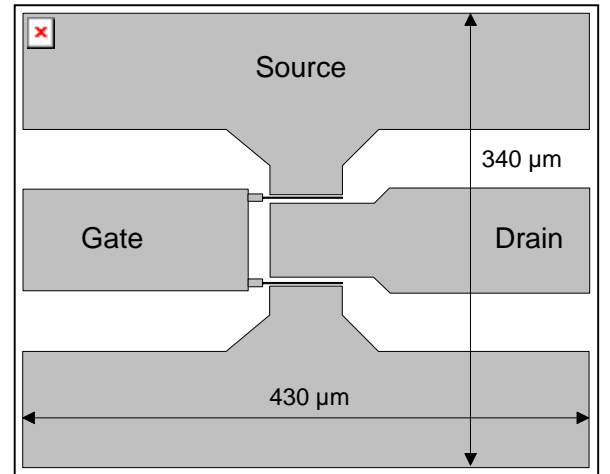


Figure 3: Layout of a $2 \times 50 \mu m$ HFET

4. RESULTS AND VERIFICATION.

The calculated output characteristics of the $Al_{0.25}Ga_{0.75}N/GaN$ -HFET are represented in Figure 4. In Figure 5 the transfer characteristic and the corresponding transconductance are plotted. To obtain a sufficient pinch-off behavior acceptor-like traps ($10^{14}cm^{-3}$) are assumed within the GaN buffer layer. The comparisons with experimental results show a good agreement.

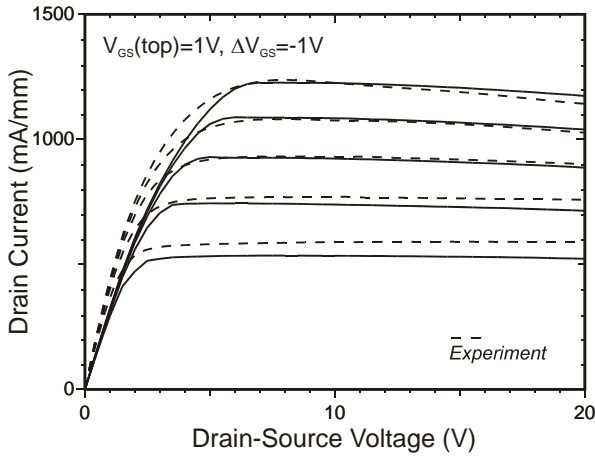


Figure 4: Output characteristics - Simulation and experimental results

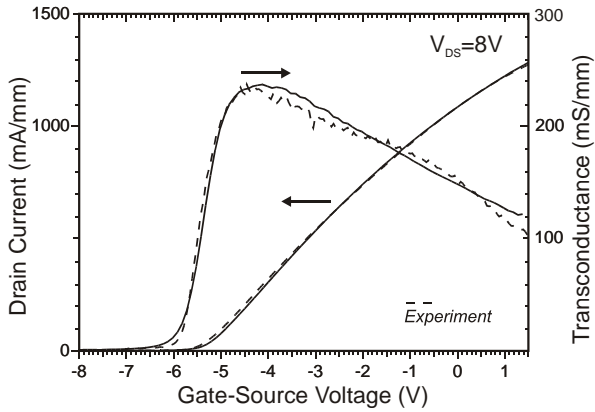


Figure 5: Transfer characteristics and transconductance - Simulation and experimental results

The computed RF-gains of the HFET are represented in Figure 6. The cut-off frequencies $f_t = 38$ GHz and $f_{max} = 64$ GHz agree with the experimental results. If the external parasitic elements are neglected the calculation of MSG/MAG and thus f_{max} yields too large values. On the other hand potentialities for improvement of RF-behavior are demonstrated.

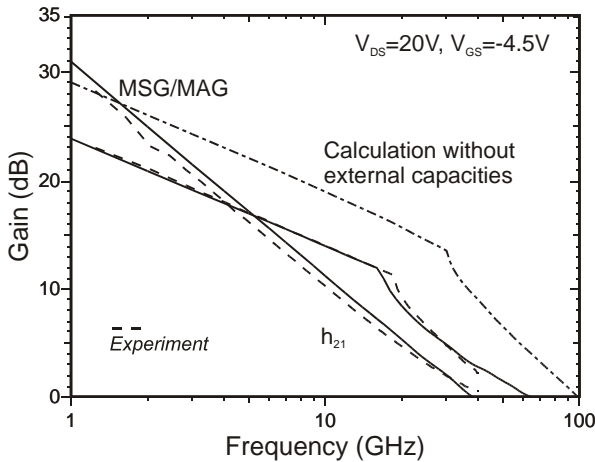


Figure 6: RF-gains versus frequency - Simulation and experimental results

5. STRUCTURE VARIATIONS

In the following different device parameters are varied to study the influence on DC and RF performance. In Figure 7 the transfer characteristics at different gate lengths in the range from $0.1 \mu\text{m}$ to $0.4 \mu\text{m}$ are represented. The drain current at a fixed gate-source voltage increases and the threshold voltages are decreased from -5.3V to -8V . At very small gate lengths the pinch-off behavior is declined.

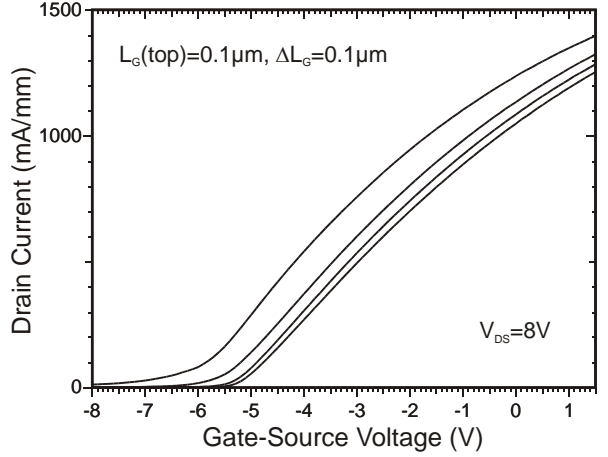


Figure 7: Transfer characteristics at different gate lengths

The RF-gains at the different gate lengths are plotted in Figure 8. The cut-off frequencies are ranged between $f_{max} = 59$ GHz - 80 GHz and $f_t = 32$ GHz - 70 GHz for $L_G = 0.4 \mu\text{m}$ - $0.1 \mu\text{m}$, respectively. At frequencies above 12 GHz higher gains can be obtained at smaller gate lengths.

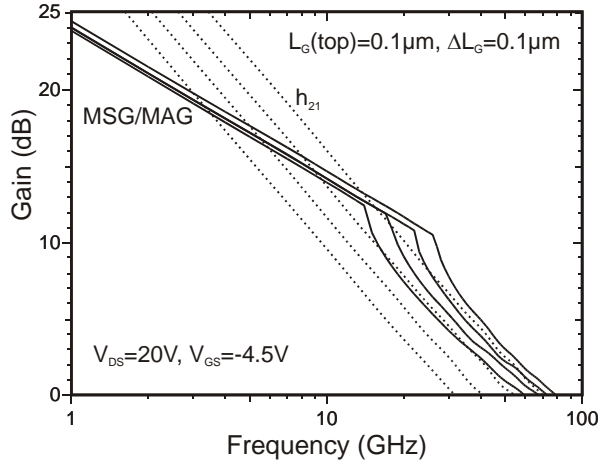


Figure 8: RF-gains at different gate lengths

The influence of the gate-drain distance L_{GD} on MSG/MAG is depicted in Figure 9. Large distances are important for high breakdown voltages. An appreciable decrease can not be determined for gate-drain distances up to $2 \mu\text{m}$. At larger values the gains and consequently f_{max} are reduced.

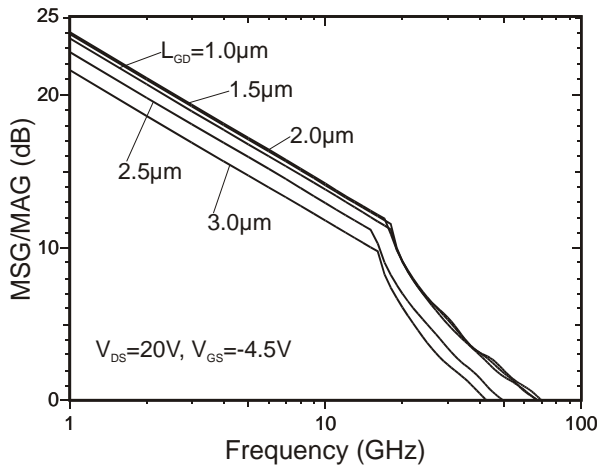


Figure 9: MSG/MAG at different gate-drain distance

Figures 10 and 11 show the transfer characteristics, the transconductance and MSG/MAG at different thickness (d_{AlGaN}) of the doped AlGaN layer. A higher thickness results in a larger gate-channel distance and an increasing electron density and consequently in an increasing drain current. The maximum of transconductance is displaced to more negative gate-source voltages and is reduced by the decreasing gate to channel aspect ratio.

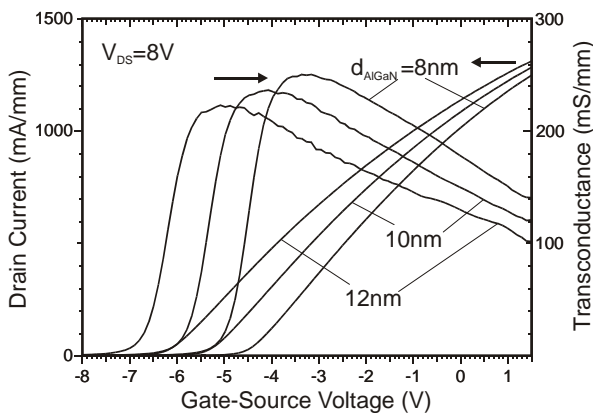


Figure 10: Transfer characteristics and transconductance at different thickness of the doped AlGaN layer

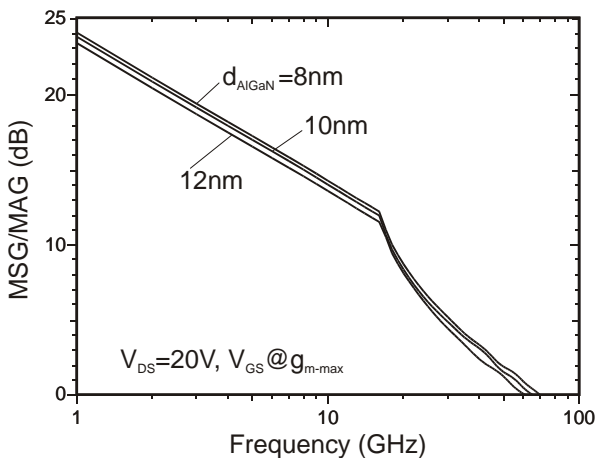


Figure 11: MSG/MAG at different thickness of the doped AlGaN layer

The RF-gains which are calculated at the maximum of transconductance ($g_{m\text{-max}}$) are in the same magnitude. The maximum frequency of oscillation varied between 61 GHz and 70 GHz for $d_{\text{AlGaN}} = 12\text{nm}$ and 8nm , respectively.

6. CONCLUSIONS

Numerical simulations of AlGaN/GaN-HFETs have been carried out. Polarization effects and self-heating processes are taken into account. The calculation of RF-gains is done in consideration of external layout elements to get realistic results. The comparison with experimental results shows good agreement both for DC and RF data. The variation of structure parameters results in hints for devices optimization. Cut-off frequencies $f_{\text{max}} = 80\text{ GHz}$ and $f_t = 70\text{ GHz}$ can be reached for a gate length $L_G = 0.1\text{ }\mu\text{m}$.

REFERENCES

- [1] R. Stenzel, C. Pigorsch, W. Klix, A. Vescan and H. Leier, "Simulation of AlGaN/GaN-HFETs including spontaneous and piezoelectric polarization charges", Inst. Phys. Conf. Ser., No.166, IOP Publishing, pp.511-514
- [2] K.-H. Rooch, A. Lerch, R. Stenzel and W. Klix, "An approach for small-signal models for RF on CMOS application with consideration of substrate influence", Proc. of 2001 IEEE Int. Analog VLSI Workshop, Bangkok 2001, pp. 107-111
- [3] J. Höntschel, R. Stenzel, W. Klix, F. Ertel, T. Asperger, R.A. Deutschmann, M. Bichler and G. Abstreiter, "Simulation of vertical CEO-FETs by a coupled solution of the Schrödinger equation with a hydrodynamic transport model", in "Simulation of Semiconductor Processes and Devices 2001", Springer-Verlag, 2001, pp. 222-225
- [4] O. Ambacher, J. Smart, J.R. Shealy, N.G. Weimann, K. Chu, M. Murphy, W.J. Schaff, L.F. Eastman, R. Dimitrov, L. Wittmer, M. Stutzmann, W. Rieger and J. Hilsenbeck, "Two-dimensional electron gases induced by spontaneous and piezoelectric polarization charges in N- and G-face AlGaIn/GaN heterostructures", J. Appl. Phys., **85** (1999), No. 6, pp. 3222-3233